

property by using AFM with an in-situ observation by using LCM-DIM. We chose hen-egg white (HEW) lysozyme as a model crystal because we can control the damage of the crystal surface by using AFM cantilever. One study was to determine the minimum force for making a hole on the surface by nano-indentation.

Seed crystals of lysozyme were prepared by a batch method. Six times re-crystallized egg-white lysozyme (Seikagaku Kogyo Co. Ltd.) was used without further purification. The buffer solution was 50mM sodium acetate (pH 4.5) and the precipitant was 25 mg/ml NaCl. Supersaturated lysozyme solution of 120 mg/ml was incubated at 20 °C for 24 hours. The small seed tetragonal crystals grew in the solution. Some seed crystals with the mother liquid were placed on a cover glass in a thermal controlling cell with 60 mg/ml lysozyme solution.

The method for operating the hybrid microscope was almost the same as our previous study [1]. We used a hard AFM cantilever (NCH, NanoWorld). The spring constant of the cantilever was about 35 N/m. Sensitivity of AFM piezoelectric device was determined by the slope of force curve of a glass plate and was about 25 nm/V. Then the approaching force was calculated by their product, which was about 0.9  $\mu\text{N/V}$ . We operated the AFM in a contact mode. The cantilever firstly positioned 50  $\mu\text{m}$  above the surface. Then we approached the cantilever with different forces between 0.09-1.8  $\mu\text{N}$ . The cantilever approached, stayed for 5 sec, and retracted. We observed the surface using LCM-DIM during the process.

We obtained the following results: Stronger force enabled us to observe a small spot (about 50 nm in diameter) where the cantilever tip was placed. This spot was disappeared after several ten seconds. The boundary force was different between increasing and decreasing the force. The observation of spot started from 1.3  $\mu\text{N}$  when the force was increased and ended at 0.5  $\mu\text{N}$  when it was decreased. This indicate that measured forces had two meanings. The value of 1.3  $\mu\text{N}$  means the force that the tip digs the crystal. On the other hand, the value of 0.5  $\mu\text{N}$  may be the crash force of the lysozyme attached on the tip.

[1] S. Yanagiya, N. Goto, *J. Cryst. Growth* **2010**, 312, 3356-3360. [2] G. Sazaki, et al., *J. Cryst. Growth* **2004**, 262, 536-542. [3] S. Yanagiya, N. Goto, *Jpn. J. Appl. Phys.* **2011**, in press.

**Keywords:** AFM, optical\_microscopy, surface\_process

## MS49.P08

*Acta Cryst.* (2011) A67, C535

### The nanoscale composite nature of biological carbonate skeletons

P. Alexa, D. Xu, X. Wang, G. Jordan, E. Griesshaber, W. W. Schmahl, Department of Earth and Environmental Sciences, LMU Theresienstr, (Germany). E-mail: patrick\_alex@web.de

In order to highlight the composite nature (Figs. 1a, 1b), the nanoscale internal structure (Figs. 1c, 1d) and the interface between the bioinorganic and polymer components in carbonate biological materials we performed dissolution experiments in an AFM cell and monitored the changes with AFM (Figs. 2a, 2b). The investigated samples were shells of modern calcitic brachiopods and the teeth and spines of modern sea urchins. By using different solutions in the AFM cell, both components, the organic as well as the inorganic component within the skeleton could be dissolved selectively (Fig. 2b). The mineral phase was dissolved by using distilled water, the organic polymers within the skeletons were digested and removed from the skeleton with the enzymes trypsin and chitinase. The resulting morphology highlighted the dissolved and the remaining undissolved components (Fig. 2b). Thus the nanoscale structure of both, the inorganic and the organic components as well as their dissolution behavior and distribution pattern in the skeleton could be highlighted and monitored in-situ.

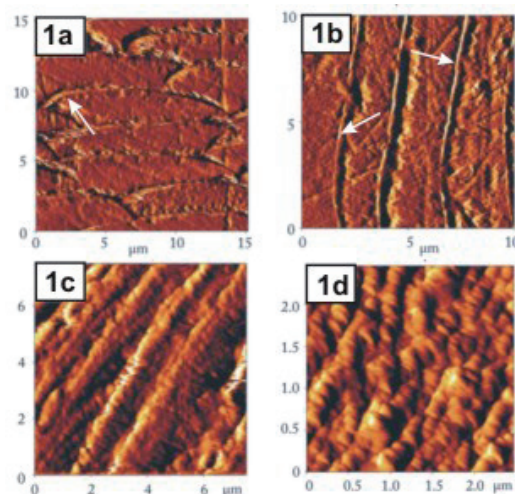


Figure 1. Arrays of transversally (1a) and longitudinally (1b) sectioned brachiopod fibres in the shell of the modern brachiopod *Magellania venosa* (1a, 1b). The fibres are lined by organic sheaths (white arrows in 1a and 1b) and have an internal granular nanostructure (1d).

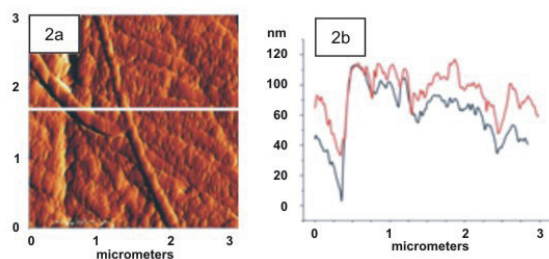


Figure 2. Dissolution of brachiopod calcite for 1 hour by distilled water. Fig. 2b shows the height of the sample at the position of the white line in Fig. 2a before (red graph in 2b) and after (black graph in 2b) the dissolution experiment. The difference in height shows that water has dissolved the calcite phase in contrast to the organic sheaths around the fibres.

**Keywords:** nanostructure, organic inorganic interface, AFM.

## MS49.P09

*Acta Cryst.* (2011) A67, C535-C536

### Step interlacing on the (100) face of retgersite crystal

Elena Petrova, Moscow State University, Moscow (Russian Federation). E-Mail: petrova@polly.phys.msu.ru

Step interlacing phenomenon is natural for a number of organic and inorganic crystals. It is known step interlacing interpretations of F. Frank [1] and W.van Enckevort [2]. But question of dislocation spiral formation was left out so far.

The central part of growth hillock on the (001) face of retgersite crystal ( $\text{NiSO}_4 \cdot 6\text{H}_2\text{O}$ ) was visualized by in-situ AFM method.

The model of dislocation spiral formation with step interlacing is proposed in this work. It is based on rectangular critical nucleus turn in accordance with screw symmetry axis of fourth order. Thickness of each of 4 layers is equal to  $\frac{1}{4}$  parameter  $c$ . The center of turning serves as asymmetrical equilibrium point of Wulf's theorem. Different speed anisotropy of layers causes the separation of fast lower layer from slow upper one and the brakeage of fast upper layer on slow lower one. In chime with experiment on hillock slope in echelon steps have height of unit  $c$  and at angles of polygonized hillock interlacing steps have heights of  $\frac{1}{4}$  and  $\frac{3}{4}$  unit  $c$ , correspondingly.

[1]. F. Frank, *Philos.Mag.* **1951**, *42*, 1014-1021. [2]. W. van Enckevort, P. Bennema, *ActaCryst.* **2004**, *A60*, 532-541.

**Keywords:** growth, nickel sulfate

## MS49.P10

*Acta Cryst.* (2011) **A67**, C536

### When does the chirality of NaClO<sub>3</sub> crystals arise in solution growth?

Hiromasa Niinomi, Katsuo Tsukamoto, Takahiro Kuribayashi, Hitoshi Miura, *Graduate School of Science, Tohoku University, (Japan)*. E-mail: h\_niinomi@s.tohoku.ac.jp

Chiral symmetry breaking in sodium chlorate (NaClO<sub>3</sub>) crystallization from a solution was reported by Kondepudi et al. (1990) [1]. The chiral NaClO<sub>3</sub> crystal has cubic crystal system and space group of  $P2_13$ . When Kondepudi et al. evaporated NaClO<sub>3</sub> solution without any mechanical disturbance, they obtained equal numbers of L- and D-crystals in the solution. In contrast, from a stirred solution almost only one type of crystals was obtained. This significant bias in chirality is termed as chiral symmetry breaking. Some theoretical models have been proposed for the mechanism of the chiral symmetry breaking, however, the mechanism has not been elucidated yet. To obtain the direct evidence of chiral symmetry breaking, we carried out in-situ observation of the crystallization process by using a polarization microscope. As a result, we found that non-cubic metastable crystals appeared at first, and then, transformed to cubic crystals by a solid-solid phase transition or a solution-mediated phase transition [2].

On the assumption that the metastable crystal is achiral, we conclude that the chirality of NaClO<sub>3</sub> crystal arises when the phase transition occurs. However, it is unknown whether the metastable crystal is chiral or achiral because the crystal structure has not been analyzed in the literature till date. Thus, in the present paper, we reported the result of a single-crystal X-ray diffraction experiment for the metastable crystal.

The metastable crystal was prepared by drop evaporation method as follows. A drop (6  $\mu$ l) of a NaClO<sub>3</sub> solution saturated at room temperature (293K) was put onto a cover glass. The metastable phase crystallized in the drop as the solution evaporated. After the crystal grew up to 200  $\mu$ m in size, the drop were replaced with glycerin. Afterwards, the crystal and the drop of glycerin were frozen by liquid nitrogen. The frozen drop is the specimen for the X-ray diffraction experiment. X-ray diffraction data was collected in oscillation mode by imaging plate type single-crystal X-ray diffractometer (R-AXIS IV++, Rigaku). To keep specimen frozen during the experiment, we kept the temperature around the specimen at  $-266\pm 1$  K by Cryostream (Oxford).

From the X-ray diffraction, we determined the lattice constant, crystal system, and space group of the metastable phase as follows;  $a=8.42$  (Å),  $b=5.26$  (Å),  $c=6.70$  (Å),  $\beta=109.71^\circ$ , monoclinic, and  $P2_1/a$ , respectively. These values are very similar to that of NaClO<sub>3</sub>(I), which was reported as a high temperature phase of NaClO<sub>3</sub> crystal in melt growth ( $a=8.78$  (Å),  $b=5.17$  (Å),  $c=6.83$  (Å),  $\beta=110^\circ$ ), monoclinic, and  $P2_1/a$  [3]. Therefore, it is highly possible that the metastable phase we obtained from the solution is the same as the NaClO<sub>3</sub>(I) phase. In addition, we found that the metastable crystal is achiral because a crystal having a space group of  $P2_1/a$  is achiral. From these results, we concluded that chirality of the cubic NaClO<sub>3</sub> crystal arises when the phase transition occurs.

The achiral metastable crystals have not been considered in the NaClO<sub>3</sub> crystallization from the solution. The phase transition from the achiral phase to the chiral phase may lead to a new understanding for the chiral symmetry breaking.

[1] D.K. Kondepudi, R.J. Kaufman, N. Singh, *Science* **1990**, *250*, 975-976. [2] H. Niinomi, K. Tsukamoto, M. Uwaha, H. Miura, *Japan Geoscience Union*

*Meeting 2010*, MIS012-06. [3] P. Meyer, M. Gasperin, *Bull. Soc. Fr. Mineral. Cristallogi* **1973**, *96*, 18-20.

**Keywords:** solution growth, chiral symmetry breaking, low temperature in-situ single crystal X-ray diffraction

## MS49.P11

*Acta Cryst.* (2011) **A67**, C536-C537

### Functionalized ZnO nanostructures for gas sensing and photovoltaic applications

Andrea Zappettini,<sup>a</sup> Davide Calestani,<sup>a</sup> Laura Lazzarini,<sup>a</sup> Marco Villani,<sup>a</sup> Filippo Fabbri,<sup>a</sup> Lucio Zanotti,<sup>a</sup> Nicola Coppedè,<sup>b</sup> Marco Nardi,<sup>b</sup> Salvatore Iannotta,<sup>a,b</sup> <sup>a</sup>IMEM-CNR, Parma (Italy). <sup>b</sup>IMEM-CNR, Trento (Italy). E-mail: zapp@imem.cnr.it

Zinc oxide (ZnO) is an incredibly versatile material that in its nanostructured form is studied for a large number of applications in optoelectronics, photovoltaics, gas and bio-sensing, piezoelectric devices, photocatalysis, spintronics, etc.

Recently this group has successfully reported the optimized not-catalyzed synthesis processes for producing single morphologies of ZnO nanostructures (i.e. nanowires [1], aligned nanorods [2], and nanotetrapods [3]) among the many different ones that are generally obtained in vapor phase reactions. The proper combination of metal thermal evaporation and controlled oxidation has produced good quality nanostructures, whose properties were not affected by contamination from catalysts or precursors.

The great potential of these nanostructures, however, can be fully explored only once they are functionalized with different organic or inorganic materials for tailoring their intrinsic properties towards the final application.

In this work authors report some meaningful examples of surface functionalization of their ZnO nanostructures by inorganic (calcogenides) and organic (phthalocyanines and porphyrins) semiconductors for applications in gas sensing, photovoltaics and photocatalytic degradation of water and gas pollutants. Although different techniques were used (an optimized chemical bath deposition – CBD – process and a supersonic molecular beam deposition – SuMBD – apparatus), in both cases particular attention has been devoted to the interface formation in the coupled compounds, in order to obtain working heterostructures where charge carriers can be efficiently separated and transferred.

The obtained functionalized ZnO nanostructures have been characterized accurately by electron microscopy (SEM and TEM), x-ray diffraction (XRD) and optical measurements (optical absorption, photoluminescence, and cathodoluminescence). The heterostructures properties have been also studied by functional characterizations such as chemoresistive gas sensing tests, photocurrent and photocatalytic activity measurements. The correlation between structural and functional properties has then been discussed.

In the case of functionalization with CdS, for example, a thickness dependent effect of charge transfer to the ZnO nanostructure has been demonstrated, together with an enhancement of the photocatalytic properties, and the modification of the gas sensing response mechanisms.

In the case of functionalization with organics, different emission spectra have been observed together with different morphologies of the obtained depositions. These phenomena have been discussed in terms of distinct molecular bonding of phthalocyanines and porphyrins at the interface with the oxide nanostructures.

[1] M. Zha, D. Calestani, A. Zappettini, R. Mosca, M. Mazzera, L. Lazzarini, L. Zanotti, *Nanotechnology* **2008**, *19*, 325603. [2] D. Calestani, M. Zha, L. Zanotti, M. Villani, A. Zappettini, *CrystEngComm* **2011**, *13*, 1707-1712. [3]